Inorganic Chemistry

COMMUNICATION

pubs.acs.org/IC

Construction of Polyoxometalate-Based Inorganic−Organic Compounds Using Silver(I) Double Helicates as Secondary Building Blocks

Dongbin Dang, Guangshui Zheng, Yan Bai,* Fan Yang, Hui Gao, Pengtao Ma, and Jingyang Niu*

Institute of Molecular and Crystal Engineering, School of Chemistry and Chemical Engineering, Henan University, Kaifeng 475004, China

Supporting Information

ABSTRACT: Two polyoxometalate-based silver(I) compounds including a three-dimensional porous crystalline array and a double-helicate bisupporting cluster were achieved using metal−organic helicates and Keggin $[PMo_{12}O_{40}]^{3-}$ as secondary building blocks.

The design and construction of multifunctional porous materials is currently of great interest because of their potential applications in several technological areas such as molecular adsorption and separation processes, heterogeneous catalysis, and artificial storage.[1] Polyoxometalates (POMs) are regarded as one kind of outstanding inorganic building blocks for the synthesis of inorganic−organic hybrid materials because of their attractive discrete, nanometer-sized, electronic, and molecular properties.[2,3] These solid materials are attractive to chemists not only for their variety of topologies and intriguing frameworks but also for their attractive electric, magnetic, catalytic, and optical properties.[4,5] One of the remarkable approaches in the design of functionalized materials based on POMs is to utilize the incorporation between polyoxoanions and different transition-metal complexes.

On the other hand, the use of discrete molecular units in the assembly of open porous frameworks is an attractive synthetic approach because the structural integrity of the building units can be maintained throughout the reaction, and the desired physical properties can be imparted to solid-state materials.[6] Helicates, which are composed of one or more covalent organic strands wrapped around a series of ions defining the helical axis, are one kind of excellent discrete building blocks for the assembly of chiral materials from achiral components.[7] Using metal helicates to synthesize POM-based porous structures is more attractive given the following considerations: (i) The basic features of the design necessary to assemble metal helices are now fairly well established, allowing us to probe systematically the effect of metal helical second building units (SBUs) through which we are attempting to control the precise topography of the complexes. (ii) The large size of metal helicate could result in porous structures with high rigidity and without a tendency to interpenetrate. (iii) Because the selected helicates are ionic species, the electrostatic interactions driven by the POM anions are an essential factor influencing molecular formation and crystallization. (iv) The intrinsically chiral character of helicates provided an opportunity to translate chirality from one helicate to others and to achieve the complicated chiral species.[8,9] Therefore, this strategy is anticipated to obtain POM-based large porous structures with metal helicates acting as SBUs, even to realize spontaneous resolution of chiral helicates at the supramolecular level. While a number of POM-based hybrid materials have been assembled by the reactions of different transition-metal organic units with POMs,[10] the use of metal helicates as SBUs to construct a POM-based multifunctional composite is still lacking.[11]

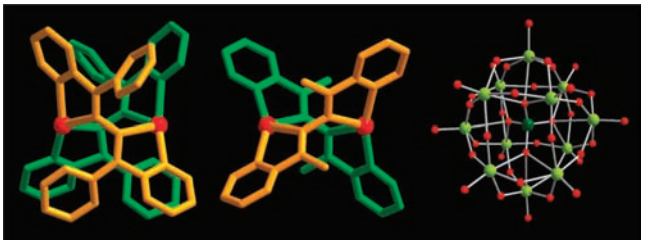

Figure 1. Ball-and-stick representations of silver(I) double helicate: $[Ag_2L^1{}_2]^{2+}$ (left), $[Ag_2L^2{}_2]^{2+}$ (middle), and Keggin $[PMo_{12}O_{40}]^{3-}$ (right).

The L^1 and L^2 chosen here have been used to assemble the anion-dependent silver helicates in previous reports.[12,13] As part of our studies on the construction of chiral metal−organic species and POM-based compounds,[5,9] in this paper we report the synthesis and characterization of two interesting POM-based inorganic−organic hybrid materials constructed from silver(I) double helicates and a $[PMo_{12}O_{40}]^{3-}$ cluster (Figure 1). The compounds referred to include a three-dimensional (3D) porous crystalline array, $[Ag_2L^1{}_2]_6(PMo_{12}O_{40})_4\cdot 5DMF\cdot 3H_2O$ (**1**), and a double helicate bisupporting cluster, $[(PMo_{12}O_{40})(Ag_2L^2{}_2)_2]OH\cdot 3H_2O$ (**2**). To the best of our knowledge, **1** is the first example of a POM-based large porous compound with discrete metal helicates as building blocks.

Single-crystal structural analyses for **1** and **2** have unequivocally confirmed that both of them are constructed from double-helical architectures and $[PMo_{12}O_{40}]^{3-}$ anions (Figures 2 and 3).[14] Compound **1** crystallizes in a centrosymmetric space group $P\bar{1}$; consequently, there are three double-metal helices $[Ag_2L^1{}_2]^{2+}$, one and two half $[PMo_{12}O_{40}]^{3-}$ anions with a phosphorus atom lying at the symmetric center (Figure S1 in the Supporting Information, SI). The silver centers exhibit ΔΔ[Ag(1), Ag(2)], ΔΔ[Ag(3), Ag(4)], and ΛΛ[Ag(5), Ag(6)] absolute configurations. In other words, there are two *P* helicates and one *M* helicate in the current

Received: January 25, 2011
Published: August 09, 2011

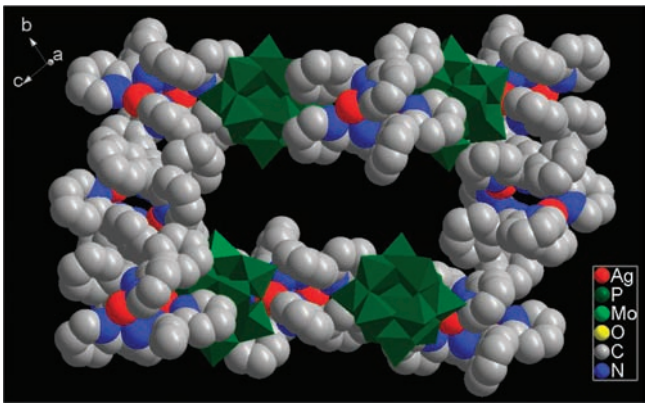

Figure 2. Molecular packing of compound **1** showing the large void. The solvent molecules are omitted for clarity. Average Ag−N bond distances (Å): Ag(1)−N 2.355(15), Ag(2)−N 2.363(13), Ag(3)−N 2.339(12), Ag(4)−N 2.368(12), Ag(5)−N 2.349(12), Ag(6)−N(17) 2.354(11).

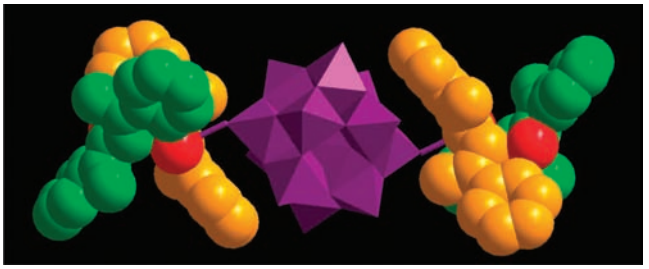

Figure 3. Polyhedral and space-filling packing representation of the double-helicate bisupporting cluster $[(PMo_{12}O_{40})(Ag_2L^2_2)_2]$ in **2**. Selected bond distances (Å): Ag(1)−N(1) 2.251(8), Ag(1)−N(2) 2.432(8), Ag(1)−N(7) 2.454(10), Ag(1)−N(8) 2.254(10), Ag(1)−O(4) 2.687(8), Ag(2)−N(3) 2.413(8), Ag(2)−N(4) 2.252(8), Ag(2)−N(5) 2.220(10), Ag(2)−N(6) 2.517(10).

asymmetric unit (Figure S2 in the SI). For each helical cation, the two silver centers are coordinated by two coupled ligands with Ag···Ag separations of 4.69 Å for Ag(1)···Ag(2), 4.64 Å for Ag(3)···Ag(4), and 4.66 Å for Ag(5)···Ag(6). Each silver ion is coordinated to two imine and two pyridyl nitrogen atoms, forming a distorted tetrahedral geometry. There are weak coordination interactions between the silver atom Ag(5) and the oxygen atom O(67C) of the $[PMo_{12}O_{40}]^{3-}$ anion with a Ag···O distance of 2.71 Å (symmetry code C: $-x, -y, 1-z$). Additional C−H···N hydrogen bonds are found in the double-helical architecture and also play an important role in stabilizing the structure (Table S4 in the SI).

As expected, it is interesting to note that **1** is a porous 3D framework with cooperative intermolecular multiform C−H···O hydrogen bonds (Figures 2 and S3 in the SI). The low density of $\rho_c = 1.865\ g\cdot cm^{-3}$ compared to that of **2** ($\rho_c = 2.357\ g\cdot cm^{-3}$) and the analogue ($\rho_c = 2.04\ g\cdot cm^{-3}$),[11] suggested a porous structure. Taking account of the larger-pore structural feature for **1**, a *PLATON* program analysis indicates that approximately 11% of the crystal volume becomes available to the solvents, and the value increases to 30% after removal of the lattice solvent molecules. It is worth noting that intermolecular interactions have the potential to assemble smaller and simpler fragments into desired cavities under favorable conditions, which is important in host−guest chemistry and has applications in chemistry, biology, and materials science.

As shown in Figure 3, **2** shows one $[PMo_{12}O_{40}]^{3-}$ supporting two silver(I) double helicates. **2** crystallizes in centrosymmetric space group $P\bar{1}$; consequently, the two supporting double helicates occur as a racemic mixture of ΛΛ and ΔΔ configuration enantiomers, whereby the equivalent fragments are interrelated by the inversion center of the phosphorus atom (Figure S4 in the SI). The helicate consists of two silver(I) ions chelated and bridged by two L^2 with a Ag(1)···Ag(2) separation of 4.64 Å. The five-coordinated Ag(1) ion exhibits a triangular-bipyramidal configuration, which is defined by one terminal oxygen atom from the $[PMo_{12}O_{40}]^{3-}$ core with a Ag(1)−O(4) distance of 2.687(8) Å and four nitrogen atoms of the two pyridylimine units. Ag(2) is coordinated by two pyridylimine units from each of the two ligands to form a tetrahedron configuration. The imine nitrogen atoms form hydrogen bonds with the carbon atoms of the methyl groups, stabilizing the helical structure.

Intermolecular $\pi-\pi$ stacking interactions between the pyridyl ring [C(15)−C(19)N(5)] and the symmetry-related ring from an adjacent molecule (symmetry code: $1+x, 2+y, 2+z$) link the double-helicate bisupporting clusters one-by-one to form one-dimensional infinite chains with a centroid−centroid separation of 3.76 Å and a shortest interplanar atom···atom separation of 3.65 Å (Figure S5 in the SI). Otherwise, multiform C−H···O hydrogen bonds are found in the network and also play an important role in stabilizing the network (Table S7 in the SI).

Despite the fact that both the rigidity of the ligands and the close proximity of the two metal centers seem to be unfavorable for the formation of helicates, the absolute configurations of the two metal centers in each molecule are identical. The nonplanar bridging mode in double helicates with two pyridylimine units linked by a single −N−N− might be essential for such kinds of ligands to encode metal ions in the formation of helicates.[8] In this paper, the dihedral angles of the two pyridine rings of the ligands are in the ranges of 81−91° for **1** and 74° and 85° for **2**, which are similar to those in related helical compounds.[12,13] Consequently, these results indicate that metal helicates as building blocks are larger in size and very stable in structure in the presence of POMs, which is helpful for making multifunctional porous compounds.

The X-ray photoelectron spectrometry spectra give two peaks at 232.1 and 235.2 eV for **1** and 232.3 and 235.4 eV for **2**, ascribed to Mo^{6+} $3d_{5/2}$ and Mo^{6+} $3d_{3/2}$, respectively (Figures S7 and S8 in the SI). The results indicate that all of the molybdenum centers in the two compounds are in the 6+ oxidation state.

The luminescent properties of two compounds have been investigated in the solid state at room temperature. Upon excitation at 220 nm, two compounds also exhibit solid-state emission spectra. Compound **1** shows emission bands at 318, 378, and 396 nm, while L^1 exhibits emission bands at 322, 372, and 395 nm (Figure S7 in the SI). Compound **2** shows emission peaks at 335 and 397 nm, while the emission peaks of ligand L^2 are at 314 and 395 nm (Figure S8 in the SI). In addition, two metal helicates exhibit emission bands at 332, 379, and 396 nm for $[Ag_2L^1_2](NO_3)_2$ and 321 and 397 nm for $[Ag_2L^2_2](NO_3)_2$ upon excitation at 220 nm. Compared to that of the corresponding ligands L^1 and L^2, the two compounds and metal helicates themselves both exhibit weaker fluorescence signals, which have been commonly observed in other Schiff base complexes.[15]

Although the identical phase of the bulk sample was confirmed by X-ray photoelectron diffraction measurements, the most intense peaks observed in the patterns are consistent with those

calculated from single-crystal diffraction data (Figure S11 in the SI). The Brunauer−Emmett−Teller measurements for **1** have been performed several times, but none of them was successful. This may be due to the existence of plenty of intermolecular interactions, making it very difficult to remove the solvent molecules from **1** under mild conditions.

In conclusion, two POM-based silver(I) compounds were achieved based on metal helicates and a Keggin $[PMo_{12}O_{40}]^{3-}$ cluster, and their fluorescent emissions in the solid state at room temperature have been determined. Not only the POM ions but also the silver(I) helicates maintained their structural integrity in the final products. This strategy is to make use of the incorporation of secondary building blocks including large silver(I) double helicates and POMs in the fascinating hybrid materials and from which the synthesizing porous framework has been realized. Studies on the assembly of other types of metal helicates and POMs and control of the chirality transfer between helicates are currently underway.

■ ASSOCIATED CONTENT

Supporting Information. Physical measurements, crystallographic data in CIF format, and the emission spectra of compounds **1** and **2**. This material is available free of charge via the Internet at http://pubs.acs.org.

■ AUTHOR INFORMATION

Corresponding Author

*E-mail: baiyan@henu.edu.cn; jyniu@henu.edu.cn.

■ ACKNOWLEDGMENT

We gratefully acknowledge financial support from the National Natural Science Foundation of China, the China Postdoctoral Science Foundation, the Foundation for University Youth Key Teacher of Henan Province, and the Foundation Co-established by the Province and the Ministry of Henan University.

■ REFERENCES

(1) (a) Furukawa, H.; Ko, N.; Go, Y. B.; Aratani, N.; Choi, S. B.; Choi, E.; Yazaydin, A.; Snurr, R. Q.; O'Keefe, M.; Kim, J.; Yaghi, O. M. *Science* **2010**, *329*, 424–428. (b) Kawamichi, T.; Haneda, T.; Kawano, M.; Fujita, M. *Nature* **2009**, *461*, 633–635. (c) Horcajada, P.; Chalati, T.; Serre, C.; Gillet, B.; Sebrie, C.; Baati, T.; Eubank, J. F.; Heurtaux, D.; Clayette, P.; Kreuz, C.; Chang, J. S.; Hwang, Y. K.; Marsaud, V.; Bories, P.-N.; Cynober, L.; Gil, S.; Férey, G.; Couvreur, P.; Gref, R. *Nat. Mater.* **2010**, *9*, 172–178.

(2) (a) Pope, M. T. *Heteropoly- and Isopolyoxometalates*; Springer-Verlag: New York, 1983. (b) Pope, M. T. Polyoxoanions: Synthesis and Structure. *Comprehensive Coordination Chemistry II*; Wedd, A. G., Ed.; Elsevier Science: New York, 2004; Vol. 4, pp 635−678. (c) Pope, M. T., Müller, A., Eds. *Polyoxometalate Chemistry: From Topology Via Self-Assembly to Applications*; Kluwer: Dordrecht, The Netherlands, 2001. (d) Hill, C. L. Polyoxometalates: Reactivity. *Comprehensive Coordination Chemistry II*; Wedd, A. G., Ed.; Elsevier Science: New York, 2004; Vol. 4, pp 679−759.

(3) (a) Horike, S.; Dincă, M.; Tamaki, K.; Long, J. R. *J. Am. Chem. Soc.* **2008**, *130*, 5854–5855. (b) Pradeep, C. P.; Misdrahi, M. F.; Li, F. Y.; Zhang, J.; Xu, L.; Long, D. L.; Liu, T. B.; Cronin, L. *Angew. Chem., Int. Ed.* **2009**, *48*, 8309–8313. (c) Long, D. L.; Tsunashima, R.; Cronin, L. *Angew. Chem., Int. Ed.* **2010**, *49*, 1736–1758. (d) Mitchell, S. G.; Streb, C.; Miras, H. N.; Boyd, T.; Long, D. L.; Cronin, L. *Nat. Chem.* **2010**, *2*, 308–312. (e) Pradeep, C. P.; Long, D. L.; Cronin, L. *Dalton Trans.* **2010**, *39*, 9443–9457.

(4) (a) Kikukawa, Y.; Yamaguchi, K.; Mizuno, N. *Angew. Chem., Int. Ed.* **2010**, *49*, 6096–6100. (b) Xiao, F. P.; Hao, J.; Zhang, J.; Lv, C. L.; Yin, P. C.; Wang, L. S.; Wei, Y. G. *J. Am. Chem. Soc.* **2010**, *132*, 5956–5957. (c) Duan, C. Y.; Wei, M. L.; Guo, D.; He, C.; Meng, Q. J. *J. Am. Chem. Soc.* **2010**, *132*, 3321–3330. (d) Sun, C. Y.; Liu, S. X.; Liang, D. D.; Shao, K. Z.; Ren, Y. H.; Su, Z. M. *J. Am. Chem. Soc.* **2009**, *131*, 1883–1888. (e) Kong, X. J.; Ren, Y. P.; Zheng, P. Q.; Long, Y. X.; Long, L. S.; Huang, R. B.; Zheng, L. S. *Inorg. Chem.* **2006**, *45*, 10702–10711.

(5) (a) Dang, D. B.; Bai, Y.; He, C.; Wang, J.; Duan, C. Y.; Niu, J. Y. *Inorg. Chem.* **2010**, *49*, 1280–1282. (b) Dang, D. B.; Gao, H.; Bai, Y.; Hu, X. F.; Yang, F.; Niu, J. Y. *Inorg. Chem. Commun.* **2010**, *13*, 37–41.

(6) (a) Inagaki, S.; Guan, S.; Ohsuna, T.; Terasak, O. *Nature* **2002**, *416*, 304–307. (b) Rosi, N. L.; Eckert, J.; Eddaoudi, M.; Vodak, D. T.; Kim, J.; O'Keeffe, M.; Yaghi, O. M. *Science* **2003**, *300*, 1127–1130. (c) Bai, Y.; He, G. J.; Zhao, Y. G.; Duan, C. Y.; Dang, D. B.; Meng, Q. J. *Chem. Commun.* **2006**, 1530–1532.

(7) (a) Piguet, C.; Bernardinelli, G.; Hopfgartner, G. *Chem. Rev.* **1997**, *97*, 2005–2062. (b) Constable, E. C. *Comprehensive Supramolecular Chemistry*; Sauvage, J. P., Ed.; Elsevier: Oxford, U.K., 1996; Vol. 9, pp 213−252. (c) Nitschke, J. R. *Acc. Chem. Res.* **2007**, *40*, 103–112.

(8) He, C.; Zhao, Y. G.; Guo, D.; Lin, Z. H.; Duan, C. Y. *Eur. J. Inorg. Chem.* **2007**, 3451–3463.

(9) (a) Bai, Y.; Duan, C. Y.; Cai, P.; Dang, D. B.; Meng, Q. J. *Dalton Trans.* **2005**, 2678–2680. (b) Sun, Q. Z.; Bai, Y.; He, G. J.; Duan, C. Y.; Lin, Z. H.; Meng, Q. J. *Chem. Commun.* **2006**, 2777–2779. (c) Dang, D. B.; Wu, P. Y.; He, C.; Xie, Z.; Duan, C. Y. *J. Am. Chem. Soc.* **2010**, *132*, 14321–14323.

(10) (a) Lan, Y. Q.; Li, S. L.; Su, Z. M.; Shao, K. Z.; Ma, J. F.; Wang, X. L.; Wang, E. B. *Chem. Commun.* **2008**, 58–60. (b) Streb, C.; Tsunashima, R.; MacLaren, D. A.; McGlone, T.; Akutagawa, T.; Nakamura, T.; Scandurra, A.; Pignataro, B.; Gadegaard, N.; Cronin, L. *Angew. Chem., Int. Ed.* **2009**, *48*, 6490–6493. (c) Ritchie, C.; Moore, E. G.; Speldrich, M.; Kögerler, P.; Boskovic, C. *Angew. Chem., Int. Ed.* **2010**, *49*, 7702–7705. (d) Lan, Y. Q.; Li, S. L.; Wang, X. L.; Shao, K. Z.; Du, D. Y.; Zang, H. Y.; Su, Z. M. *Inorg. Chem.* **2008**, *47*, 8179–8187. (e) An, H. Y.; Wang, E. B.; Xiao, D. R.; Li, Y. G.; Su, Z. M.; Xu, L. *Angew. Chem., Int. Ed.* **2006**, *45*, 904–908. (f) Wu, Q.; Li, Y. G.; Wang, Y. H.; Clérac, R.; Lu, Y.; Wang, E. B. *Chem. Commun.* **2009**, 5743–5745.

(11) Wei, M. L.; Sun, R. P.; Zhuang, P. F.; Yang, Y. H. *Russ. J. Coord. Chem.* **2009**, *35*, 885–890.

(12) (a) Tuna, F.; Hamblin, J.; Jackson, A.; Clarkson, G.; Alcock, N. W.; Hannon, M. J. *Dalton Trans.* **2003**, 2141–2148. (b) Hambin, J.; Jackson, A.; Alcock, N. W.; Hannon, M. J. *Dalton Trans.* **2002**, 1635–1641. (c) Guo, D.; Pang, K. L.; Duan, C. Y.; He, C.; Meng, Q. J. *Inorg. Chem.* **2002**, *41*, 5978–5985.

(13) (a) Wu, C. Y.; Lee, C. S.; Pal, S.; Hwang, W. S. *Polyhedron* **2008**, *27*, 2681–2687. (b) Tuna, F.; Clarkson, G.; Alcock, N. W.; Hannon, M. J. *Dalton Trans.* **2003**, 2149–2155. (c) Guo, D.; He, C.; Duan, C. Y.; Qian, C. Q.; Meng, Q. J. *New J. Chem.* **2002**, *26*, 796–802.

(14) Crystal data of **1** for $C_{303}H_{257}Ag_{12}Mo_{48}N_{53}O_{168}P_4$: M_r = 13352.06, triclinic, $P\bar{1}$, a = 14.990(1) Å, b = 18.055(1) Å, c = 45.102(2) Å, α = 97.67(1)°, β = 91.76(1)°, γ = 100.22(1)°, V = 11887.2(11) Å^3; Z = 1; ρ_{calcd} = 1.865 g·cm^{-3}; T = 293(2) K. The final refinement gave R1 = 0.0869, wR2 = 0.1721, and GOF = 1.07 for 17 768 observed reflections with $I > 2\sigma(I)$. Crystal data of **2** for $C_{56}H_{63}Ag_4Mo_{12}N_{16}O_{44}P$: M_r = 3277.90, triclinic, $P\bar{1}$, a = 11.382(1) Å, b = 15.464(2) Å, c = 15.891(2) Å, α = 112.08(1)°, β = 105.53(1)°, γ = 104.10(1)°, V = 2304.1(4) Å^3; Z = 1; ρ_{calcd} = 2.357 g·cm^{-3}; T = 293(2) K. The final refinement gave R1 = 0.0604, wR2 = 0.1471, and GOF = 1.038 for 5090 observed reflections with $I > 2\sigma(I)$.

(15) (a) Bai, Y.; Gao, H.; Dang, D. B.; Guo, X. Y.; An, B.; Shang, W. L. *CrystEngComm* **2010**, *12*, 1422–1432. (b) Wu, H. C.; Thanasekaran, P.; Tsai, C. H.; Wu, J. Y.; Huang, S. M.; Wen, Y. S.; Lu, K. L. *Inorg. Chem.* **2006**, *45*, 295–303. (c) Dong, Y. B.; Wang, L.; Ma, J. P.; Zhao, X. X.; Shen, D. Z.; Huang, R. Q. *Cryst. Growth Des.* **2006**, *6*, 2475–2485.